

Constraints on the Gluon Density from Lepton Pair Production

E. L. Berger^{a*} and M. Klasen^{b†}

^aHEP Theory Group, Argonne National Laboratory, 9700 South Cass Avenue, Argonne, IL 60439, USA

^bII. Institut für Theoretische Physik, Universität Hamburg, Luruper Chaussee 149, D-22761 Hamburg, Germany

The hadroproduction of lepton pairs with mass Q and finite transverse momentum Q_T is described in perturbative QCD by the same partonic subprocesses as prompt photon production. We demonstrate that, like prompt photon production, lepton pair production is dominated by quark-gluon scattering in the region $Q_T > Q/2$. This feature leads to sensitivity to the gluon density in kinematical regimes accessible in collider and fixed target experiments, and it provides a new independent method for constraining the gluon density.

1. INTRODUCTION

The production of lepton pairs in hadron collisions $h_1 h_2 \rightarrow \gamma^* X; \gamma^* \rightarrow l\bar{l}$ proceeds through an intermediate virtual photon via $q\bar{q} \rightarrow \gamma^*$, and the subsequent leptonic decay of the virtual photon. Traditionally, interest in this Drell-Yan process has concentrated on lepton pairs with large mass Q which justifies the application of perturbative QCD and allows for the extraction of the antiquark density in hadrons [1].

Prompt photon production $h_1 h_2 \rightarrow \gamma X$ can be calculated in perturbative QCD if the transverse momentum Q_T of the photon is sufficiently large. Because the quark-gluon Compton subprocess is dominant, $gq \rightarrow \gamma X$, this reaction provides essential information on the gluon density in the proton at large x [2]. Unfortunately, the analysis suffers from fragmentation, isolation, and intrinsic transverse momentum uncertainties. Alternatively, the gluon density can be constrained from the production of jets with large transverse momentum at hadron colliders [3], but the information from different experiments and colliders is ambiguous.

In this paper we demonstrate that, like prompt photon production, lepton pair production is dominated by quark-gluon scattering in the region $Q_T > Q/2$. This realization means that new independent constraints on the gluon density may be derived from Drell-Yan data in kinematical regimes that are accessible in collider and fixed target experiments but without the theoretical and experimental uncertainties present in the prompt photon case.

In Sec. 2, we review the relationship between vir-

tual and real photon production in hadron collisions in next-to-leading order QCD. In Sec. 3 we present our numerical results, and Sec. 4 is a summary.

2. NEXT-TO-LEADING ORDER QCD FORMALISM

In leading order (LO) QCD, two partonic subprocesses contribute to the production of virtual and real photons with non-zero transverse momentum: $q\bar{q} \rightarrow \gamma^{(*)}g$ and $gq \rightarrow \gamma^{(*)}q$. The cross section for lepton pair production is related to the cross section for virtual photon production through the leptonic branching ratio of the virtual photon $\alpha/(3\pi Q^2)$. The virtual photon cross section reduces to the real photon cross section in the limit $Q^2 \rightarrow 0$.

The next-to-leading order (NLO) QCD corrections arise from virtual one-loop diagrams interfering with the LO diagrams and from real emission diagrams. At this order $2 \rightarrow 3$ partonic processes with incident gluon pairs (gg), quark pairs (qq), and non-factorizable quark-antiquark ($q\bar{q}_2$) processes contribute also. Singular contributions are regulated in $n=4-2\epsilon$ dimensions and removed through $\overline{\text{MS}}$ renormalization, factorization, or cancellation between virtual and real contributions. An important difference between virtual and real photon production arises when a quark emits a collinear photon. Whereas the collinear emission of a real photon leads to a $1/\epsilon$ singularity that has to be factored into a fragmentation function, the collinear emission of a virtual photon yields a finite logarithmic contribution since it is regulated naturally by the photon virtuality Q . In the limit $Q^2 \rightarrow 0$ the NLO virtual photon cross section reduces to the real photon cross section if this logarithm is replaced by a $1/\epsilon$ pole. A more detailed discussion can be found in [4].

The situation is completely analogous to hard photo-production where the photon participates in the scattering in the initial state instead of the final state. For

*Supported by the U.S. Department of Energy, Division of High Energy Physics, under Contract W-31-109-ENG-38.

†Supported by Bundesministerium für Bildung und Forschung under Contract 05 HT9GUA 3, by Deutsche Forschungsgemeinschaft under Contract KL 1266/1-1, and by the European Commission under Contract ERBFMRXCT980194.

real photons, one encounters an initial-state singularity that is factored into a photon structure function. For virtual photons, this singularity is replaced by a logarithmic dependence on the photon virtuality Q [5].

A remark is in order concerning the interval in Q_T in which our analysis is appropriate. In general, in two-scale situations, a series of logarithmic contributions will arise with terms of the type $\alpha_s^n \ln^n(Q/Q_T)$. Thus, if either $Q_T \gg Q$ or $Q_T \ll Q$, resummations of this series must be considered. For practical reasons, such as event rate, we do not venture into the domain $Q_T \gg Q$, and our fixed-order calculation should be adequate. On the other hand, the cross section is large in the region $Q_T \ll Q$. In previous papers [4], we compared our cross sections with available fixed-target and collider data on massive lepton-pair production, and we were able to establish that fixed-order perturbative calculations, without resummation, should be reliable for $Q_T > Q/2$. At smaller values of Q_T , non-perturbative and matching complications introduce some level of phenomenological ambiguity. For the goal we have in mind, viz., constraints on the gluon density, it would appear best to restrict attention to the region $Q_T \geq Q/2$, but below $Q_T \gg Q$.

3. PREDICTED CROSS SECTIONS

In this section we present numerical results for the production of lepton pairs in $p\bar{p}$ collisions at the Tevatron with center-of mass energy $\sqrt{S} = 1.8$ and 2.0 TeV. We analyze the invariant cross section $Ed^3\sigma/dp^3$ averaged over the rapidity interval $-1.0 < y < 1.0$. We integrate the cross section over various intervals of pair-mass Q and plot it as a function of the transverse momentum Q_T . Our predictions are based on a NLO QCD calculation [6] and are evaluated in the $\overline{\text{MS}}$ renormalization scheme. The renormalization and factorization scales are set to $\mu = \mu_f = \sqrt{Q^2 + Q_T^2}$. If not stated otherwise, we use the CTEQ4M parton distributions [7] and the corresponding value of Λ in the two-loop expression of α_s with four flavors (five if $\mu > m_b$). The Drell-Yan factor $\alpha/(3\pi Q^2)$ for the decay of the virtual photon into a lepton pair is included in all numerical results.

In Fig. 1 we display the NLO QCD cross section for lepton pair production at the Tevatron at $\sqrt{S} = 1.8$ TeV as a function of Q_T for four regions of Q . The regions of Q have been chosen to avoid resonances, *i.e.* between 2 GeV and the J/ψ resonance, between the J/ψ and the Υ resonances, above the Υ 's, and a high mass region. The cross section falls both with the mass of the lepton pair Q and, more steeply, with its transverse momentum Q_T . No data are available

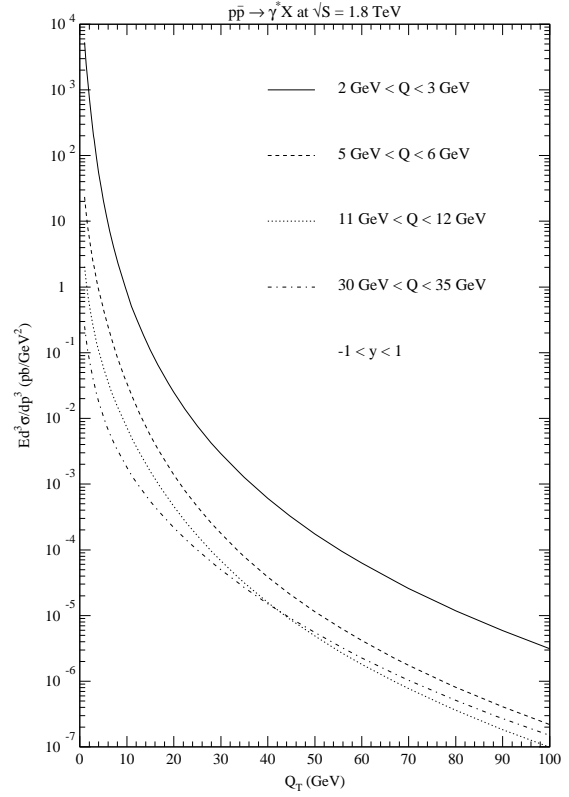


Figure 1. Invariant cross section $Ed^3\sigma/dp^3$ as a function of Q_T for $p\bar{p} \rightarrow \gamma^*X$ at $\sqrt{S} = 1.8$ TeV in non-resonance regions of Q . The cross section falls with the mass of the lepton pair Q and, more steeply, with its transverse momentum Q_T .

yet from the CDF and D0 experiments. However, prompt photon production data exist to $Q_T \simeq 100$ GeV, where the cross section is about 10^{-3} pb/GeV². It should be possible to analyze Run I data for lepton pair production to at least $Q_T \simeq 30$ GeV where one can probe the parton densities in the proton up to $x_T = 2Q_T/\sqrt{S} \simeq 0.03$. The UA1 collaboration measured the transverse momentum distribution of lepton pairs at $\sqrt{S} = 630$ GeV up to $x_T = 0.13$ [8], and their data agree well with our theoretical results [4].

The fractional contributions from the qg and $q\bar{q}$ subprocesses through NLO are shown in Fig. 2. It is evident that the qg subprocess is the most important subprocess as long as $Q_T > Q/2$. The dominance of the qg subprocess diminishes somewhat with Q , dropping from over 80 % for the lowest values of Q to about 70 % at its maximum for $Q \simeq 30$ GeV. In addition, for very large Q_T , the significant luminosity associated with the valence dominated \bar{q} density in $p\bar{p}$ reactions begins to raise the fraction of the cross section attributed to the

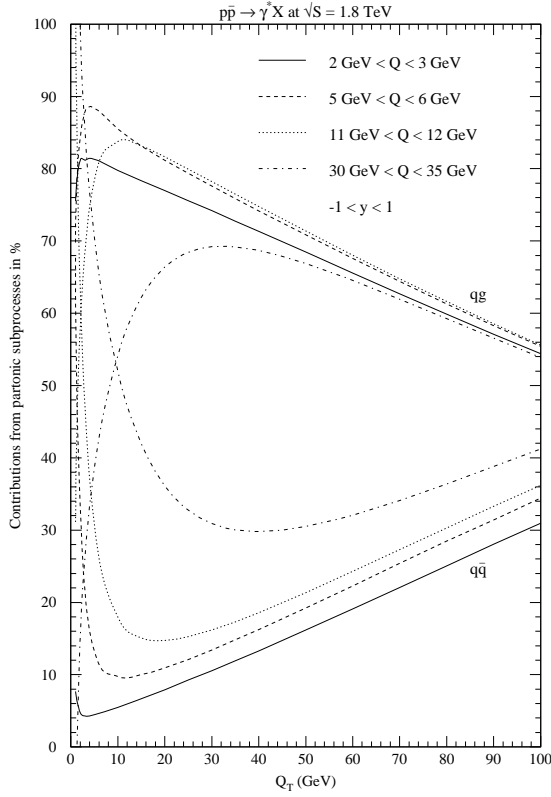


Figure 2. Contributions from the partonic subprocesses $q\bar{q}$ and $q\bar{q}$ to the invariant cross section $Ed^3\sigma/dp^3$ as a function of Q_T for $p\bar{p} \rightarrow \gamma^* X$ at $\sqrt{S} = 1.8$ TeV. The $q\bar{q}$ channel dominates in the region $Q_T > Q/2$.

$q\bar{q}$ subprocesses. Subprocesses other than those initiated by the $q\bar{q}$ and $q\bar{q}$ initial channels are of negligible import.

We update the Tevatron center-of-mass energy to Run II conditions ($\sqrt{S} = 2.0$ TeV) and use the latest global fit by the CTEQ collaboration (5M). Figure 3 demonstrates that the larger center-of-mass energy increases the invariant cross section for the production of lepton pairs with mass $5 \text{ GeV} < Q < 6 \text{ GeV}$ by 5 % at low $Q_T \simeq 1 \text{ GeV}$ and 20 % at high $Q_T \simeq 100 \text{ GeV}$. In addition, the expected luminosity for Run II of 2 fb^{-1} should make the cross section accessible to $Q_T \simeq 100 \text{ GeV}$ or $x_T \simeq 0.1$. This extension would constrain the gluon density in the same regions as prompt photon production in Run I.

Next we present a study of the sensitivity of collider and fixed target experiments to the gluon density in the proton. The full uncertainty in the gluon density is not known. Here we estimate this uncertainty from the variation of different recent parametrizations. We

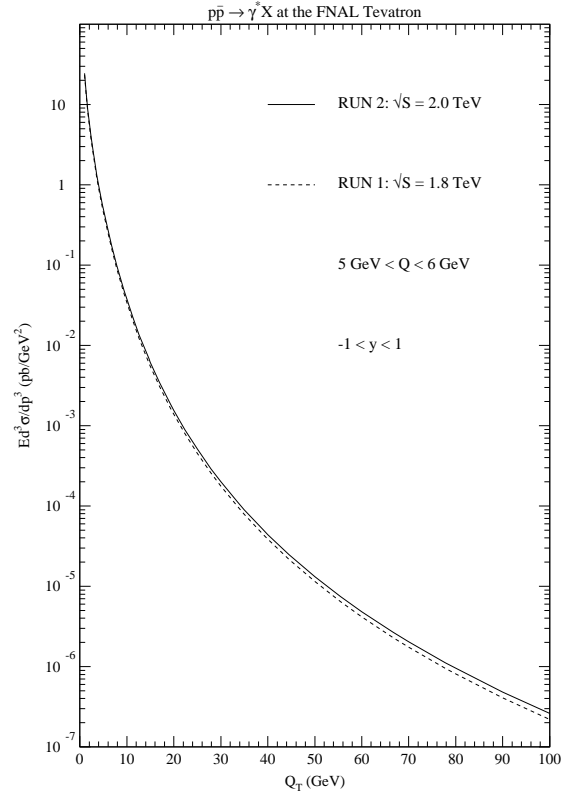


Figure 3. Invariant cross section $Ed^3\sigma/dp^3$ as a function of Q_T for $p\bar{p} \rightarrow \gamma^* X$ and two different center-of-mass energies of the Tevatron (Run 1: $\sqrt{S} = 1.8$ TeV, Run 2: $\sqrt{S} = 2.0$ TeV). The cross section for Run 2 is 5 to 20 % larger, depending on Q_T .

choose the latest global fit by the CTEQ collaboration (5M) as our point of reference [3] and compare results to those based on their preceding analysis (4M [7]) and on a fit with a higher gluon density (5HJ) intended to describe the CDF and D0 jet data at large transverse momentum. We also compare to results based on global fits by MRST [2], who provide three different sets with a central, higher, and lower gluon density, and to GRV98 [9]¹.

In Fig. 4 we plot the cross section for lepton pairs with mass between the J/ψ and Υ resonances at Run II of the Tevatron in the region between $Q_T = 10$ and 30 GeV ($x_T = 0.01 \dots 0.03$). For the CTEQ parametrizations we find that the cross section increases from 4M to 5M by 2.5 % ($Q_T = 30 \text{ GeV}$) to 5 % ($Q_T = 10$

¹In this set a purely perturbative generation of heavy flavors (charm and bottom) is assumed. Since we are working in a massless approach, we resort to the GRV92 parametrization for the charm contribution [10] and assume the bottom contribution to be negligible.

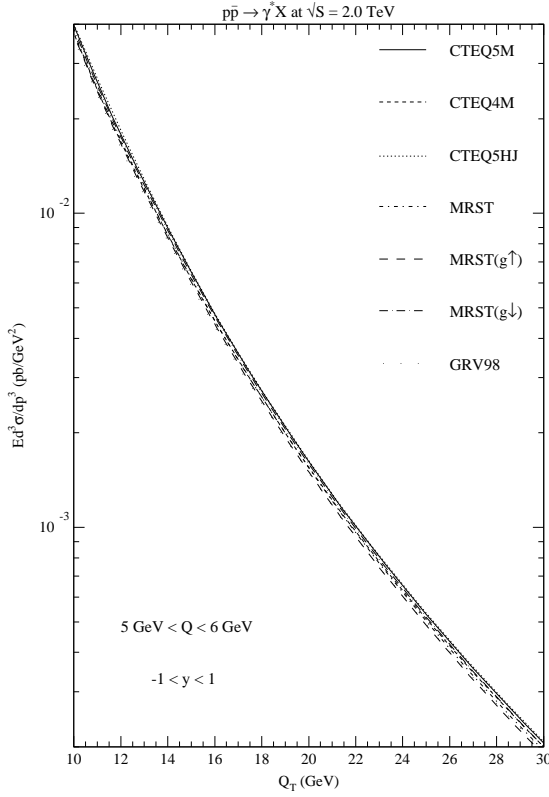


Figure 4. Invariant cross section $Ed^3\sigma/dp^3$ as a function of Q_T for $p\bar{p} \rightarrow \gamma^* X$ at $\sqrt{S} = 2.0$ TeV in the region between the J/ψ and Υ resonances. The largest differences from CTEQ5M are obtained with GRV98 at low Q_T (minus 10 %) and with MRST($g\uparrow$) at large Q_T (minus 7 %).

GeV) and from 5M to 5HJ by 1 % in the whole Q_T -range. The largest differences from CTEQ5M are obtained with GRV98 at low Q_T (minus 10 %) and with MRST($g\uparrow$) at large Q_T (minus 7%).

The theoretical uncertainty in the cross section can be estimated by varying the renormalization and factorization scale $\mu = \mu_f$ around the central value $\sqrt{Q^2 + Q_T^2}$. Figure 5 shows this variation for $p\bar{p} \rightarrow \gamma^* X$ at $\sqrt{S} = 2.0$ TeV in the region between the J/ψ and Υ resonances. In the interval $0.5 < \mu/\sqrt{Q^2 + Q_T^2} < 2$ the dependence of the cross section on the scale $\mu = \mu_f$ drops from $\pm 15\%$ (LO) to the small value $\pm 2.5\%$ (NLO). The K -factor ratio (NLO/LO) is approximately 2, as one might expect naively.

A similar analysis for Fermilab's fixed target experiment E772 [11] is shown in Fig. 6. In this experiment, a deuterium target is bombarded with a proton beam of momentum $p_{\text{lab}} = 800$ GeV, *i.e.* $\sqrt{S} = 38.8$ GeV. The cross section is averaged over the scaled longitu-

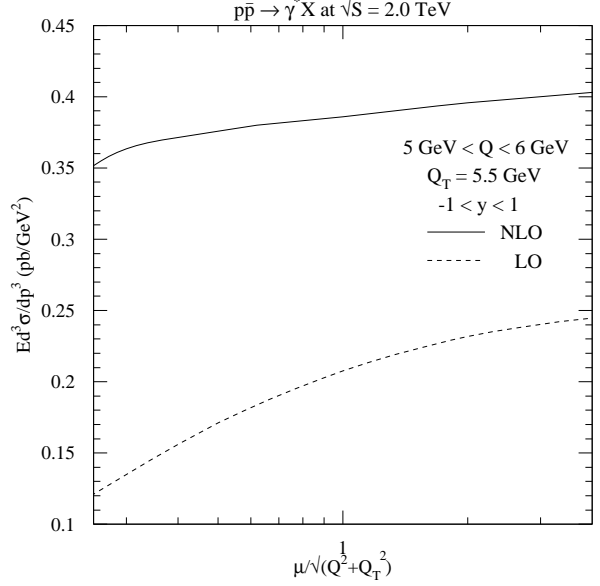


Figure 5. Invariant cross section $Ed^3\sigma/dp^3$ as a function of the renormalization and factorization scale $\mu = \mu_f$ for $p\bar{p} \rightarrow \gamma^* X$ at $\sqrt{S} = 2.0$ TeV in the region between the J/ψ and Υ resonances and $Q_T = 5.5$ GeV. In the interval $0.5 < \mu/\sqrt{Q^2 + Q_T^2} < 2$ the dependence of the cross section on the scale $\mu = \mu_f$ drops from $\pm 15\%$ (LO) to $\pm 2.5\%$ (NLO). The K -Factor (NLO/LO) is approximately 2.

dinal momentum interval $0.1 < x_F < 0.3$. In fixed target experiments one probes substantially larger regions of x_T than in collider experiments. Therefore one expects greater sensitivity to the gluon distribution in the proton. We find that use of CTEQ5HJ increases the cross section by 7 % (26 %) w.r.t. CTEQ5M at $Q_T = 3$ GeV ($Q_T = 6$ GeV) and by 134 % at $Q_T = 10$ GeV. With MRST($g\downarrow$) the cross section drops relative to the CTEQ5M-based values by 17 %, 40 %, and 59 % for these three choices of Q_T .

Figure 7 shows the variation of the fixed target cross section on the renormalization and factorization scale $\mu = \mu_f$. In the interval $0.5 < \mu/\sqrt{Q^2 + Q_T^2} < 2$ the dependence decreases from $\pm 49\%$ (LO) to $\pm 37\%$ (NLO). An optimal scale choice might be $\mu = \mu_f = \sqrt{Q^2 + Q_T^2}/4$, where the points of Minimal Sensitivity (maximum of NLO) and of Fastest Apparent Convergence (LO=NLO) nearly coincide. At $\mu = \mu_f = \sqrt{Q^2 + Q_T^2}$, the K -factor ratio is 2.6. The NLO cross section turns negative at the lowest scale shown $\mu = \mu_f = \sqrt{Q^2 + Q_T^2}/8 \simeq 1$ GeV, a value too low to guarantee perturbative stability.

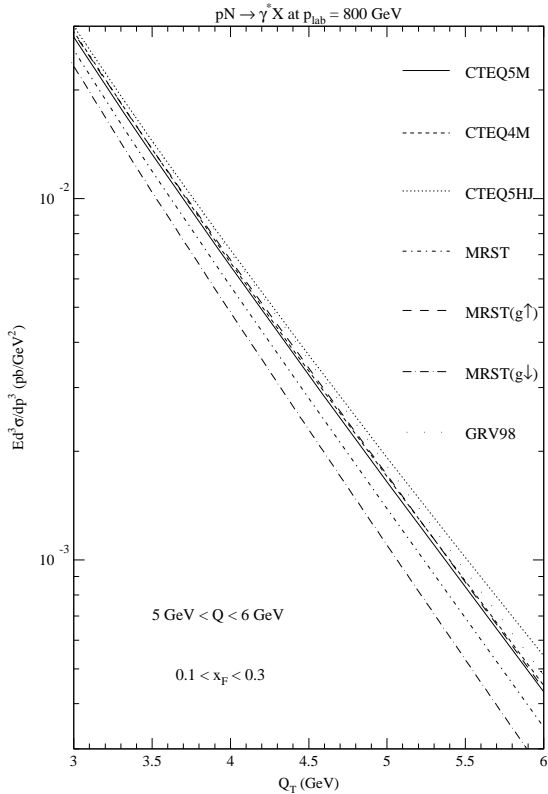


Figure 6. Invariant cross section $Ed^3\sigma/dp^3$ as a function of Q_T for $pN \rightarrow \gamma^* X$ at $p_{\text{lab}} = 800$ GeV. The cross section is highly sensitive to the gluon distribution in the proton in regions of x_T where it is poorly constrained in current analyses.

4. SUMMARY

The production of Drell-Yan pairs with low mass and large transverse momentum is dominated by gluon initiated subprocesses. In contrast to prompt photon production, uncertainties from fragmentation, isolation, and intrinsic transverse momentum are absent. The hadroproduction of low mass lepton pairs is therefore an advantageous source of information on the parametrization and size of the gluon density. The increase in luminosity of Run II increases the accessible region of x_T from 0.03 to 0.1. The theoretical uncertainty has been estimated from the scale dependence of the cross sections and found to be very small for collider experiments.

Acknowledgment

It is a pleasure to thank L. E. Gordon for his collaboration.

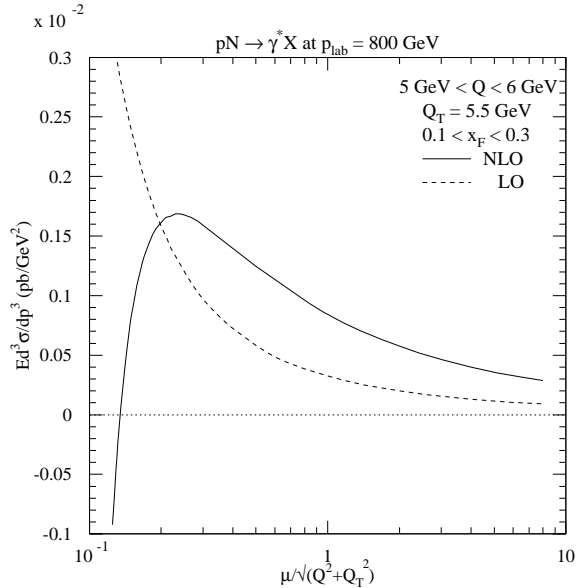


Figure 7. Invariant cross section $Ed^3\sigma/dp^3$ as a function of the renormalization and factorization scale $\mu = \mu_f$ for $pN \rightarrow \gamma^* X$ at $p_{\text{lab}} = 800$ GeV. In the interval $0.5 < \mu/\sqrt{Q^2 + Q_T^2} < 2$ the dependence of the cross section on the scale μ drops from $\pm 49\%$ (LO) to $\pm 37\%$ (NLO).

REFERENCES

1. S.D. Drell and T. Yan, Phys. Rev. Lett. **25** (1970) 316.
2. A.D. Martin, R.G. Roberts, W.J. Stirling and R.S. Thorne, Eur. Phys. J. **C4** (1998) 463, hep-ph/9803445, and hep-ph/9907231.
3. H.L. Lai *et al.* [CTEQ Collaboration], hep-ph/9903282.
4. E.L. Berger, L.E. Gordon and M. Klasen, Phys. Rev. **D58** (1998) 074012, hep-ph/9803387; E. L. Berger and M. Klasen, hep-ph/9906402.
5. M. Klasen, G. Kramer and B. Pötter, Eur. Phys. J. **C1** (1998) 261, hep-ph/9703302.
6. P.B. Arnold and R.P. Kauffman, Nucl. Phys. **B349** (1991) 381.
7. H.L. Lai *et al.*, Phys. Rev. **D55** (1997) 1280, hep-ph/9606399.
8. C. Albajar *et al.* [UA1 Collaboration], Phys. Lett. **209B** (1988) 397.
9. M. Glück, E. Reya and A. Vogt, Eur. Phys. J. **C5** (1998) 461, hep-ph/9806404.
10. M. Glück, E. Reya and A. Vogt, Z. Phys. **C53** (1992) 127.
11. P.L. McGaughey *et al.* [E772 Collaboration], Phys. Rev. **D50** (1994) 3038.